#### **ORIGINAL ARTICLE**



# A robust nickel catalyst with an unsymmetrical propyl-bridged diphosphine ligand for catalyst-transfer polymerization

Matthew A. Baker<sup>1</sup> · Josué Ayuso-Carrillo<sup>1</sup> · Martin R. M. Koos o<sup>1</sup> · Samantha N. MacMillan o<sup>2</sup> · Anthony J. Varni<sup>1</sup> · Roberto R. Gil o<sup>1</sup> · Kevin J. T. Noonan o<sup>1</sup>

Received: 7 June 2019 / Revised: 9 July 2019 / Accepted: 30 July 2019 / Published online: 3 September 2019 © The Society of Polymer Science, Japan 2019

#### **Abstract**

A new nickel diphosphine catalyst has been synthesized in which the bidentate ligand has two different phosphine donors, a typical PPh<sub>2</sub> group and a stronger  $\sigma$ -donating PEt<sub>2</sub> group. The catalyst was highly effective for the chain-growth polymerization of a 3-alkylthiophene monomer using a Suzuki–Miyaura cross-coupling. The catalyst is particularly effective for this polymerization in the presence of excess free ligand. The unsymmetrical diphosphine nickel complex reported here represents a new approach to tuning metal-ligand reactivity in the chain-growth polymerization of aromatic monomers. In addition, this new nickel catalyst exhibited increased hydrolytic resistance in the polymerization as compared to commercially available 1,3-bis(diphenylphosphino)propane nickel dichloride.

#### Introduction

Metal-catalyzed cross-couplings continue to be among the most powerful strategies for forming C–C bonds, and they are commonly employed to synthesize  $\pi$ -conjugated polymers. These reactions typically proceed by a step-growth mechanism, but an interaction between the metal catalyst and the  $\pi$ -system [1, 2] of the growing macromolecule can result in a chain-growth process (known as catalyst-transfer polymerization or CTP). This affords well-defined polymers with controllable molecular weights and narrow molecular weight distributions [3–11]. The ancillary ligand bound to the metal is critical to the chain-growth process because it governs both the metal-polymer  $\pi$ -interactions and the cross-coupling efficiency [3–11].

Of the cross-coupling reactions used for CTP, the Suzuki-Miyaura reaction is advantageous due to the functional group compatibility of organoboron moieties and the

**Supplementary information** The online version of this article (https://doi.org/10.1038/s41428-019-0259-3) contains supplementary material, which is available to authorized users.

relatively mild reaction conditions needed to promote C–C bond formation. While palladium complexes are often used to catalyze this transformation [12–24], nickel catalysts such as Ni(dppp)Cl<sub>2</sub> and Ni(IPr)(PPh<sub>3</sub>)Cl<sub>2</sub> can also be employed to polymerize X-Ar-B(OR)<sub>2</sub> monomers [25, 26]. Herein, we prepared a nickel diphosphine precatalyst with two unique phosphine donors (Scheme 1) for CTP.

The desymmetrization of the diphosphine ligand enables specific modifications of the steric and electronic environments on each donor atom bound to the metal. In this report, the bidentate ligand is composed of diaryl (PPh<sub>2</sub>) and dialkyl (PEt<sub>2</sub>) phosphines with a bridging propyl linker. This diphosphine was synthesized according to a published procedure [27–29], and it is abbreviated "split" diethyl diphenyl phosphine or sepp for simplicity. The ligand strongly binds nickel and offers improved hydrolytic resistance under basic conditions compared to commercially available 1,3-bis (diphenylphosphino)propane nickel dichloride (Ni(dppp) Cl<sub>2</sub>). Most importantly, Ni(sepp)Cl<sub>2</sub> can catalyze the controlled polymerization of a 3-hexylthiophene monomer using Suzuki-Miyaura coupling.

The polymerization catalyst is particularly effective when the reaction is conducted in the presence of excess free

 <sup>⊠</sup> Kevin J. T. Noonan noonan@andrew.cmu.edu

Department of Chemistry, Carnegie Mellon University, 4400 Fifth Avenue, Pittsburgh, PA 15213-2617, USA

Department of Chemistry and Chemical Biology, Baker Laboratory, Cornell University, Ithaca, NY 14853-1301, USA

Scheme 1 Synthesis of the Ni(sepp)Cl<sub>2</sub> precatalyst for CTP

ligand. Remarkably, although the catalyst is unsymmetric, a single catalyst resting state was identified using <sup>31</sup>P NMR spectroscopy, indicating that oxidative addition to the Ni<sup>0</sup> occurs preferentially with the growing chain *trans* to the PEt<sub>2</sub> group. An externally initiated variant of this catalyst was also synthesized and shown to be highly effective for controlling the polymer end groups. Altogether, the data suggest that individual modification of the donor ligands in bidentate structures may be a valuable ligand design strategy for chain-growth polycondensation and, more broadly, for cross-coupling reactions.

#### Materials and methods

All synthetic manipulations of air-sensitive compounds were carried out under an N2 atmosphere using standard Schlenk techniques or in an N2-filled glovebox. All glassware was dried overnight in an oven and heated under vacuum prior to use. Solvents were dried and degassed prior to use. Deionized water for the polymerizations was thoroughly degassed by a continuous flow of N<sub>2</sub> for at least 30 min. The sepp ligand was prepared according to a literature procedure [27] though a different reducing agent was used for the final step [30]. The <sup>1</sup>H and <sup>31</sup>P NMR spectra of sepp and the ligand precursors are provided in the Supporting Information (Figs. S1-S3). Monomer 1 (2-(5-bromo-4-hexylthiophen-2-yl)—4,4,5,5-tetramethyl-1,3,2-dioxaborolane) was synthesized from literature procedures with minor modifications [23, 31]. All other compounds were purchased from commercial vendors and used as received.

#### **NMR** analysis

All NMR spectra were recorded on a 500 Bruker Avance III or a 500 Bruker Avance Neo ( $^{1}$ H, 500 MHz;  $^{13}$ C, 125.8 MHz;  $^{31}$ P, 202.5 MHz) spectrometer. NMR signals were referenced to residual solvent for  $^{1}$ H and deuterated solvents for  $^{13}$ C{ $^{1}$ H}. The proton-decoupled  $^{31}$ P{ $^{1}$ H} NMR spectra were electronically referenced using internal Bruker software according to a universal scale determined from the precise ratio,  $\Xi$ , of the resonance frequency of the  $^{31}$ P nuclide to the  $^{1}$ H resonance of TMS in a dilute solution ( $\varphi$  < 1%) [32]. All polymer samples subjected to  $^{31}$ P{ $^{1}$ H} NMR analysis were prepared by removing 0.5 mL of the polymer solution and transferring it into an NMR tube housed in a Schlenk tube under  $N_2$ . Aliquots were removed from the polymerization at specific time points and analyzed.

#### Gel-permeation chromatography

Gel-permeation chromatography (GPC) measurements were performed on a Waters Instrument equipped with a 717 plus autosampler, a Waters 2414 refractive index (RI) detector, and two SDV columns (Porosity 1000 and 100,000 Å; Polymer Standard Services) with THF as the eluent (~1 mg/mL, flow rate 1 mL/min, 40 °C). A 10-point calibration based on polystyrene standards (Polystyrene, ReadyCal Kit, Polymer Standard Services) was used to determine the molecular weights.

# **MALDI-TOF** analysis

MALDI-TOF analyses were performed using an Applied Biosystems Voyager DE-STR mass spectrometer. One microliter of a solution of the matrix (*trans*-2-[3-(4-*t*-butyl-phenyl)-2-methyl-2-propenylidene]malonitrile, DCTB) in THF (10 mg/mL) was spotted onto a well of the MALDI plate, and the solvent was allowed to evaporate. Polymer sample solutions (2 mg/mL in THF) were prepared, and 1 μL of this solution was spotted onto the well by a layering method. The solvent was evaporated prior to analysis. Data were collected in positive polarity mode in either linear or reflection mode.

## X-ray analysis

Low-temperature X-ray diffraction data for (sepp)Ni (o-C<sub>6</sub>H<sub>4</sub>CO<sub>2</sub>Me)Br and Ni(sepp)Cl<sub>2</sub> were collected on a Rigaku XtaLAB Synergy diffractometer coupled to a Rigaku Hypix detector with Cu K $\alpha$  radiation ( $\lambda$  = 1.54184 Å) from a PhotonJet microfocus X-ray source at 100 K. The diffraction images were processed and scaled using CrysAlisPro software [33]. The structures were solved through intrinsic phasing using SHELXT [34] and refined against F<sup>2</sup> on all data by full-matrix least squares with SHELXL [35] following established refinement strategies [36]. All nonhydrogen atoms were refined anisotropically. All hydrogen atoms bound to carbon were included in the model at geometrically calculated positions and refined using a riding model. The isotropic displacement parameters of all hydrogen atoms were fixed to 1.2 times the Ueq value of the atoms they are linked to (1.5 times for methyl groups). Details of the data quality and a summary of the residual values of the refinements are listed in the Supporting Information (Tables S1 and S2). The crystallographic data for (sepp)Ni(o-C<sub>6</sub>H<sub>4</sub>CO<sub>2</sub>Me)Br and Ni(sepp)Cl<sub>2</sub> have been deposited with the Cambridge Crystallographic Data Center (CCDC) under the reference numbers CCDC 1911056 and 1911057, respectively. These data can be obtained free of charge via www.ccdc.cam.ac. uk/data request/cif.

#### **End-group analysis**

The degree of polymerization (DP) for each poly(3-hexylthiophene) (P3HT) sample was estimated from the alkyl region of the <sup>1</sup>H NMR spectrum [37–39]. For polymers prepared using Ni(sepp)Cl<sub>2</sub>, the α-CH<sub>2</sub> signal of the hexyl tail on the H-terminated end group (triplet at 2.62 ppm) [37, 39] was compared to the  $\alpha$ -CH<sub>2</sub> signal of the polymer (triplet centered at 2.81 ppm, integrated from 2.90 to 2.65 ppm). The H-terminated end group signal was set to 2, and the DP was calculated as follows: DP = (integration of polymer  $CH_2$  signal/2) + 1 for the Br-terminated end group +1 for the H-terminated group. For polymers prepared using (sepp)Ni(o-C<sub>6</sub>H<sub>4</sub>CO<sub>2</sub>Me)Br, the CH<sub>3</sub> signal of the o-C<sub>6</sub>H<sub>4</sub>CO<sub>2</sub>Me end group (singlet at 3.80 ppm) [38] was compared to the α-CH<sub>2</sub> signal of the polymer (triplet centered at 2.81 ppm, integration from 2.90 to 2.65 ppm). The end group signal was set to 3, and the DP was calculated as follows: DP = (integration of polymer CH<sub>2</sub> signal/2) + 1 for the H-terminated end group.

#### **Computational studies**

Density functional theory calculations were performed for all compounds using a mixed basis set with B3LYP 6–31 G (d) for all atoms in the ligand and SDD for nickel in the Gaussian 09 suite [40]. The Cartesian coordinates of the optimized geometries are available as xyz files, and the total energies of the two isomers are included in Table S3 (ESI).

#### **Experimental procedures**

## Ni(sepp)Cl<sub>2</sub>

To an oven-dried 100 mL Schlenk flask were added NiCl<sub>2</sub> (0.118 g, 0.91 mmol), sepp (0.300 g, 0.95 mmol) and degassed ethanol (15 mL) under an inert atmosphere. The suspension was stirred at 90 °C for 1 h and then cooled to 8 °C to facilitate precipitation of the target compound. The nickel dihalide complex was isolated as an air-stable, redorange solid by vacuum filtration and washed with ethanol and diethyl ether (0.140 g, 35% yield). Crystals were grown from a concentrated solution in  $\text{CH}_2\text{Cl}_2$  (~20 mg/mL) layered with *n*-hexane or diethyl ether.

<sup>31</sup>P{<sup>1</sup>H} NMR (202 MHz, CD<sub>2</sub>Cl<sub>2</sub>) δ 8 (br s, 2P). <sup>1</sup>H NMR (500 MHz, CD<sub>2</sub>Cl<sub>2</sub>) δ 7.97 (d, J = 7.4 Hz, 4H), 7.56 (t, J = 7.5 Hz, 4H), 7.50 (t, J = 7.4 Hz, 2H), 3.07 (br s, 2H), 2.48 (br s, 2H), 2.07 (br s, 2H), 1.91 (s, 2H), 1.70 (p, J = 5.8 Hz, 2H), 1.43 (t, J = 7.4 Hz, 6H). <sup>13</sup>C{<sup>1</sup>H} NMR (126 MHz, CD<sub>2</sub>Cl<sub>2</sub>): δ 135.4, 134.1 (br), 131.8, 129.2, 26.1, 23.6 (br), 20.2, 19.1, 10.5. HRMS (DART-MS) (m/z): [2M-Cl]<sup>+</sup> calculated for C<sub>38</sub>H<sub>52</sub>Cl<sub>3</sub>Ni<sub>2</sub>P<sub>4</sub>, 853.0792; found, 853.0789.

# (PPh<sub>3</sub>)<sub>2</sub>Ni(o-C<sub>6</sub>H<sub>4</sub>CO<sub>2</sub>Me)Br

In a glovebox, a scintillation vial equipped with a magnetic stir bar was charged with bis(1,5-cyclooctadiene)nickel (0.165 g, 0.6 mmol), triphenylphosphine (0.315 g, 1.20 mmol), and toluene (6 mL). After complete dissolution of the reagents in toluene, methyl-2-bromobenzoate (0.142 g, 0.66 mmol) was added into the reaction mixture, and the solution was vigorously stirred at 23 °C for 18 h, during which time a solid precipitated from the reaction mixture. The suspended solids were precipitated by hexanes (~60 mL), isolated by filtration and washed with hexanes (~200 mL) and methanol (~200 mL). The resulting brightyellow solid was dried under reduced pressure at 50 °C, affording 0.420 g (88% yield) of the nickel complex.

31P{¹H} NMR (202 MHz, CD<sub>2</sub>Cl<sub>2</sub>): δ 20.8 (s). ¹H NMR

5<sup>1</sup>P{ <sup>1</sup>H} NMR (202 MHz, CD<sub>2</sub>Cl<sub>2</sub>): δ 20.8 (s). <sup>1</sup>H NMR (500 MHz, CD<sub>2</sub>Cl<sub>2</sub>): δ 7.75–7.53 (br s, 12H), 7.50 (d, J = 7.5 Hz, 1H), 7.41–7.10 (br m, 18H), 6.68 (d, J = 7.9 Hz, 1H), 6.48 (t, J = 7.6 Hz, 1H), 6.32 (t, J = 7.4 Hz, 1H), 3.74 (s, 3H). <sup>13</sup>C{ <sup>1</sup>H} NMR (126 MHz, CD<sub>2</sub>Cl<sub>2</sub>): δ 169.5, 166.2, 136.8, 136.6, 135.1, 132.5, 131.8, 129.9, 128.9, 128.0, 121.5, 51.9. HRMS (DART-MS) (m/z): [M + H]<sup>+</sup> calculated for C<sub>44</sub>H<sub>38</sub>BrNiO<sub>2</sub>P<sub>2</sub>, 797.0884; found, 797.6169.

### (sepp)Ni(o-C<sub>6</sub>H<sub>4</sub>CO<sub>2</sub>Me)Br

In a glovebox, a scintillation vial equipped with a stir bar was charged with (PPh<sub>3</sub>)<sub>2</sub>Ni(o-C<sub>6</sub>H<sub>4</sub>CO<sub>2</sub>Me)Br (0.237 g, 0.30 mmol), sepp (0.103 g, 0.33 mmol), and THF (4.8 mL). The solution was vigorously stirred at 23 °C for 18 h, during which time a precipitate formed in the reaction mixture. The suspended solids were precipitated by hexanes (~50 mL), isolated by filtration and washed with hexanes (~150 mL). The resulting bright-yellow solid was dried under reduced pressure at 23 °C, affording 0.170 g (97% yield) of the nickel complex. Crystals were grown from a concentrated solution in CH<sub>2</sub>Cl<sub>2</sub> (~20 mg/mL) layered with *n*-hexane.  ${}^{31}P\{{}^{1}H\}$  (202 MHz, THF- $d_8$ )  $\delta$  18.0 (d,  $J_{PP}$  = 70.3 Hz, 1P), -5.7 (d,  $J_{PP} = 70.2$  Hz, 1P). <sup>1</sup>H NMR (500) MHz, THF- $d_8$ )  $\delta$  8.55 (br s, 2H), 7.59 (br s, 3H), 7.49–7.41 (m, 1H), 6.98 (dt, J = 7.7, 1.8 Hz, 2H), 6.80 (t, J = 7.7 Hz, 2H), 6.62 (tt, J = 7.4, 1.6 Hz, 1H), 6.55 (t, J = 8.9 Hz, 2H), 6.32 (t, J = 7.4 Hz, 1H), 3.81 (s, 3H), 2.53–2.31 (m, 2H; note: this signal overlaps with H<sub>2</sub>O), 2.28–2.15 (m, 1H), 2.11-1.99 (m, 2H), 1.89-1.76 (m, 1H), 1.71-1.66 (m, 2H; note: this signal overlaps with the solvent signal), 1.66–1.55 (m, 1H), 1.40 (dt, J = 15.8, 7.6 Hz, 3H), 1.30-1.19 (m, 1H),1.12 (dt, J = 14.6, 7.6 Hz, 3H). <sup>13</sup>C{<sup>1</sup>H} NMR (126 MHz, THF- $d_8$ )  $\delta$  174.6 (dd,  $J_{PC} = 79.7, 35.7 \text{ Hz}$ ), 172.3 (d,  $J_{PC} =$ 5.8 Hz), 139.2 (d,  $J_{PC} = 2.6$  Hz), 136.8 (d,  $J_{PC} = 11.9$  Hz), 135.7, 135.5 (dd,  $J_{PC} = 47.2$ , 4.6 Hz), 132.7 (d,  $J_{PC} = 44.9$ Hz), 132.2, 131.6 (d,  $J_{PC} = 7.5 \text{ Hz}$ ), 130.0 (dd,  $J_{PC} = 4.5$ , 2.5 Hz), 129.7 (d,  $J_{PC} = 5.5$  Hz), 129.5 (d,  $J_{PC} = 10.0$  Hz),

**Table 1** Preparation of P3HT using a Suzuki–Miyaura cross-coupling

Catalyst <sup>a</sup>	Addl. sepp <sup>b</sup>	DP <sub>theo</sub>	DP <sup>c</sup> (NMR)	$M_n$ (kg/mol) NMR	$M_n  (\text{kg/mol})^{\text{d}}  \text{GPC}$	Đ	Yield (%)e
Ni(sepp)Cl <sub>2</sub>	N	25	27	4.6	7.9	1.07	84
Ni(sepp)Cl <sub>2</sub>	N	50	41	6.9	14.4	1.06	74
Ni(sepp)Cl <sub>2</sub>	Y	25	26	4.4	7.8	1.07	85
Ni(sepp)Cl <sub>2</sub>	Y	50	42	7.1	13.3	1.05	70
(sepp)Ni(Ar)Br	N	25	30	5.2	6.4	1.30	80
(sepp)Ni(Ar)Br	N	50	54	9.1	10.6	1.28	88
(sepp)Ni(Ar)Br	Y	25	27	4.6	7.6	1.08	87
(sepp)Ni(Ar)Br	Y	50	55	9.3	14.9	1.05	85

 $<sup>^{</sup>a}$ All polymerizations were performed at a monomer concentration of 25 mM with 2 equiv of  $K_{3}PO_{4}\cdot H_{2}O$  and 33.33 equiv of degassed water

128.8 (d,  $J_{PC} = 2.2 \text{ Hz}$ ), 127.7 (d,  $J_{PC} = 9.5 \text{ Hz}$ ), 121.1, 51.6, 28.7 (dd,  $J_{PC} = 21.7$ , 7.9 Hz), 20.6 (dd,  $J_{PC} = 17.2$ , 3.5 Hz), 19.5 (d,  $J_{PC} = 3.5 \text{ Hz}$ ), 19.3 (d,  $J_{PC} = 24.2 \text{ Hz}$ ), 18.8 (d,  $J_{PC} = 28.1 \text{ Hz}$ ), 8.6, 8.2 (d,  $J_{PC} = 3.8 \text{ Hz}$ ). HRMS (DART-MS) (m/z): [M-Br]<sup>+</sup> calculated for  $C_{27}H_{33}NiO_{2}P_{2}$ , 509.1309; found, 509.1307.

#### Representative polymerization procedure

In a glovebox, a scintillation vial equipped with a stir bar and an open-top Teflon screw cap was charged with a calculated amount of catalyst and K<sub>3</sub>PO<sub>4</sub>·H<sub>2</sub>O (0.070 g, 0.30 mmol). In several cases (entries 3-4 and 7-8 in Table 1), a calculated amount of sepp ligand (1.0 equiv relative to catalyst) was also added to the reaction. Monomer 1 (0.056 g, 0.15 mmol) and then THF (6 mL) were added to the vial, which was then sealed and removed from the glovebox. The reaction was heated to 50 °C, and water (0.09 mL) was injected. Two hours after the addition of water, the polymerization was quenched by the addition of 6 N methanolic HCl (50 mL) with stirring for 30 min. The resulting precipitate was isolated by filtration, washed with methanol (100 mL), water (50 mL), and then methanol (200 mL) before drying. The experiment to obtain  $M_n$  versus conversion and the semilogarithmic plot was conducted according to a previous report [25].

# Results and discussion

The combination of the previously reported diphosphine [27–29] with NiCl<sub>2</sub> in refluxing ethanol (Scheme 1)

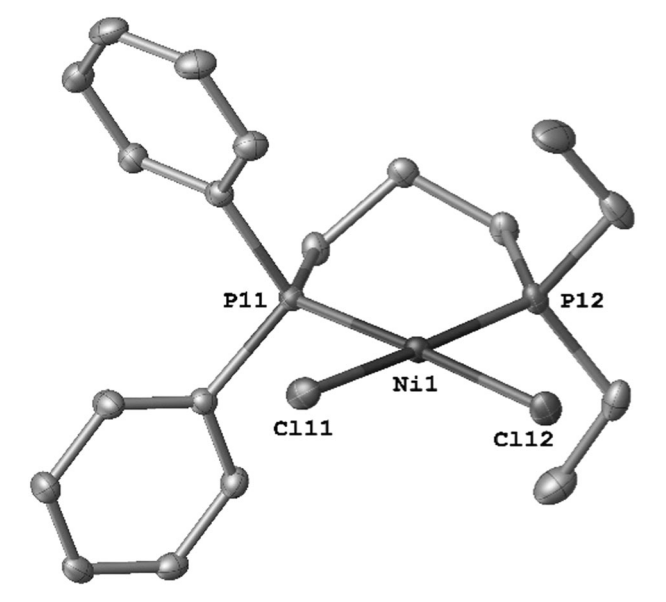


Fig. 1 Solid-state molecular structure of  $Ni(sepp)Cl_2$  (thermal ellipsoids at 50% probability) with H atoms omitted. Only one of the two independent molecules is shown

afforded Ni(sepp)Cl<sub>2</sub> in a low yield (35%). The NMR signals ( $^{1}$ H and  $^{13}$ C{ $^{1}$ H}) of the precatalyst were broad due to the very short T<sub>2</sub> relaxation times induced by the quadrupolar chlorides [41]. An extremely broad, nearly imperceptible signal was present in the  $^{31}$ P{ $^{1}$ H} NMR spectrum, presumably due to this quadrupolar relaxation. Single crystal X-ray diffraction (Fig. 1) was then employed to unambiguously assign the structure.

There are two independent molecules in the unit cell of Ni(sepp)Cl<sub>2</sub>. The average nickel–phosphine bond lengths

<sup>&</sup>lt;sup>b</sup>1.0 equiv of sepp relative to catalyst

<sup>&</sup>lt;sup>c</sup>DP was estimated using end-group analysis

<sup>&</sup>lt;sup>d</sup>GPC traces were recorded versus polystyrene standards in THF at 40 °C

<sup>&</sup>lt;sup>e</sup>Isolated yield

Scheme 2 Proposed pathway of precatalyst reduction and hydrolysis

for the two different phosphines are nearly identical (2.1609 (4) Å for the Ni-PPh<sub>2</sub> moiety and 2.1712(4) Å for the Ni-PEt<sub>2</sub> unit). Interestingly, the bite angles in the two independent precatalyst molecules differ by over 2° and average to 95°. This suggests a slightly larger steric constraint imposed by the two unique phosphines in Ni(sepp)Cl<sub>2</sub> compared to that of Ni(dppp)Cl<sub>2</sub>, in which the bite angle of the diphosphine is 91.8° [42].

Upon complete characterization of the Ni(sepp)Cl<sub>2</sub> complex, its performance in CTP was evaluated. This precatalyst was used to initiate the polymerization of a 3-alkylthiophene monomer bearing a bromine at the 2-position and a pinacol boronate at the 5 position (1) in THF with  $K_3PO_4\cdot H_2O$  as the base and minimal water at 50 °C. The concentrations of base and water used in these experiments were identical to our optimized conditions for Ni(dppp)Cl<sub>2</sub>. Using 4 mol% Ni (sepp)Cl<sub>2</sub>, P3HT with a DP of 27, an  $M_n$  of 7.9 kg/mol, and D of 1.07 (Table 1, Entry 1) was obtained.

The molecular weight and distribution of the P3HT sample suggested that Ni(sepp)Cl<sub>2</sub> was a promising catalyst for CTP, but it also raised some questions. Prior reports on the mechanism of Suzuki-Miyaura cross-coupling have indicated that ligand substitution reactions of metal-halogen bonds to form metal-hydroxo species are critical for the transmetalation with the aryl boronate [43–49]. Considering this, activation of the nickel dihalide precatalyst likely requires exchange of the Cl ligands for OH ligands prior to transmetalation and reductive elimination (depicted in Scheme 2). Consequently, this hydroxide exchange can potentially impact the efficiency of the precatalyst reduction. In our prior work on the polymerization of 1 with Ni (dppp)Cl<sub>2</sub> [25], NMR spectroscopy revealed a significant portion of free dppp in the reaction mixture. The presence of dppp likely stemmed from metal-hydroxide formation involving the precatalyst and subsequent dissociation of the diphosphine ligand to afford the catalytically inactive nickel hydroxide (proposed pathway in Scheme 2). Miyaura and

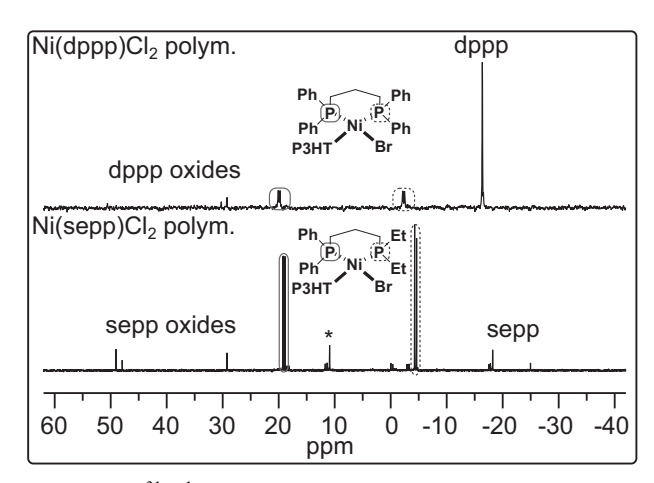


Fig. 2 Crude  $^{31}P\{^{1}H\}$  NMR spectra recorded in THF of the polymerization reaction conducted with Ni(dppp)Cl<sub>2</sub> (top) and Ni(sepp)Cl<sub>2</sub> (bottom). Aliquots were removed 60 min after initiation from 25 mM polymerizations of monomer 1 with 10 mol % catalyst, 2 equiv of  $K_3PO_4$ · $H_2O$ , and 33.3 equiv of degassed water. \* indicates unidentified side-product

coworkers have documented sensitivity of dihalide precatalysts for Suzuki-Miyaura cross-coupling in their previous work [50–52]. Although a portion of the Ni(dppp) Cl<sub>2</sub> precatalyst was lost to hydrolysis, this event was critical to the overall chain-growth polymerization process since the combination of the remaining active catalyst and free ligand were necessary to achieve the controlled polymerization, as evidenced by control experiments [25]. The hydrolysis of Ni(dppp)Cl<sub>2</sub> led us to consider whether Ni(sepp)Cl<sub>2</sub> with the stronger PEt<sub>2</sub> donor would show different precatalyst initiation behavior.

Our interrogation of the polymerization reaction using <sup>31</sup>P{<sup>1</sup>H} NMR spectroscopy revealed that Ni(sepp)Cl<sub>2</sub> was significantly more resistant to precatalyst hydrolysis when compared to Ni(dppp)Cl<sub>2</sub> (Fig. 2). For comparison, free dppp and its oxide account for nearly 60% of the integration intensity in the spectrum of an aliquot of the Ni(dppp)Cl<sub>2</sub>-initiated polymerization, while for Ni(sepp)Cl<sub>2</sub>, the free ligand and its oxide account for only 10% of the mixture. In addition to hydrolytic resistance, only one pair of doublets was observed from the major product in the Ni(sepp)Cl<sub>2</sub>-initiated polymerization (Fig. 2). The chemical shifts are close to those of the pair of doublets observed when polymerizing with Ni(dppp)Cl<sub>2</sub>.

Transmetalation has been identified as the rate-limiting step when using Ni(dppp)Cl<sub>2</sub> as the catalyst in both Kumada–Corriu- and Suzuki–Miyaura-initiated CTPs [25, 53, 54]. The resting state of the catalyst, (dppp)Ni (P3HT)Br, can be observed using  $^{31}$ P{ $^{1}$ H} NMR spectroscopy [53, 54]. The two doublets in the top of Fig. 2 correspond to this Ni<sup>2+</sup> species that has undergone oxidative addition. The downfield signal near 20 ppm ( $^{2}J_{PP}$ =

64.4 Hz) corresponds to the PPh<sub>2</sub> group *trans* to the halogen, and the upfield signal near -3 ppm corresponds to the PPh<sub>2</sub> group *trans* to the growing chain ( $^2J_{PP} = 65.8$  Hz) [55]. A similar pattern is observed for the polymerization with Ni(sepp)Cl<sub>2</sub>. One doublet appeared at 19.1 ppm ( $^2J_{PP} = 71.0$  Hz), and the other appeared further upfield at -4.5 ppm ( $^2J_{PP} = 70.9$  Hz).

The similarity to the Ni(dppp)Cl<sub>2</sub> polymerization suggested that the oxidative addition product is also the resting state of the catalyst in this case. Moreover, the upfield shift of the second signal was indicative that the more electronrich PEt<sub>2</sub> is *trans* to the growing chain. If the oxidative addition was not selective, then one would expect to see two pairs of doublets for the two possible stereoisomers. Some minor doublets are indeed observed in the spectrum, so it is likely that the other stereoisomer forms (along with several other minor species), but the major signals, are the result of the selective arrangement of the P3HT and Br around the unsymmetrical nickel catalyst.

To confirm the positions of the phosphino groups relative to the corresponding aryl bromide, a model compound was synthesized. Luscombe and co-workers [38, 56] previously synthesized an externally initiated (dppp)Ni(*o*-tolyl)Br catalyst for cross-coupling polymerizations. Unfortunately, the isolation and characterization of the analogous (sepp)Ni(*o*-tolyl)Br was unsuccessful. Methylbenzoate was considered as a replacement for the *o*-tolyl ligand since the methyl ester should be a suitable substituent to block the axial site of the nickel [57], and it can potentially coordinate to the metal via the oxygen atoms. Bis(1,5-cyclooctadiene)nickel, PPh<sub>3</sub>, and methyl 2-bromobenzoate were combined to form an airstable Ni<sup>2+</sup> complex prior to ligand exchange with sepp (Scheme 3).

The  $^{31}P\{^{1}H\}$  NMR signals for (sepp)Ni(o-C<sub>6</sub>H<sub>4</sub>CO<sub>2</sub>Me) Br were nearly identical to those observed in the spectrum obtained from the polymerization reactions. For (sepp)Ni(o-C<sub>6</sub>H<sub>4</sub>CO<sub>2</sub>Me)Br in THF- $d_8$ , signals were observed at 18.0 ppm ( $^2J_{\rm PP}=70.3$  Hz) and -5.7 ppm ( $^2J_{\rm PP}=70.2$  Hz). Two minor doublets that exchange with the major species are also observed at 4.8 and 1.9 ppm. The identity of this species is still under investigation. A 2D  $^1$ H $^{-31}$ P HMQC experiment optimized for long-range coupling (J=8 Hz) confirmed that the downfield signal near 19 ppm corresponds to the PPh<sub>2</sub> group of sepp. The correlations of the P atom to the broad protons of the phenyl rings are indicated in Fig. 3.

Scheme 3 Ligand exchange of sepp with  $PPh_3$  to prepare an externally initiated  $Ni^{2+}$  complex

The signal near -5 ppm corresponds to the PEt<sub>2</sub> group, as evidenced by the correlations to the methylene and methyl groups (marked by the blue box in Fig. 3). Notably, the phosphorus atom of the PEt<sub>2</sub> group also correlates strongly with nearly all the signals of the propyl backbone of the 6-membered metallacycle and the *trans*-2-methylbenzoate group. The assignments for (sepp)Ni(o-C<sub>6</sub>H<sub>4</sub>CO<sub>2</sub>Me)Br are consistent with those of the spectra acquired during the polymerizations (Fig. 2, bottom) and suggest an energetic preference for the reactive arene ligand being *trans* to the PEt<sub>2</sub> group.

The formation of a single stereoisomer was also confirmed for (sepp)Ni(o-C<sub>6</sub>H<sub>4</sub>CO<sub>2</sub>Me)Br using single crystal

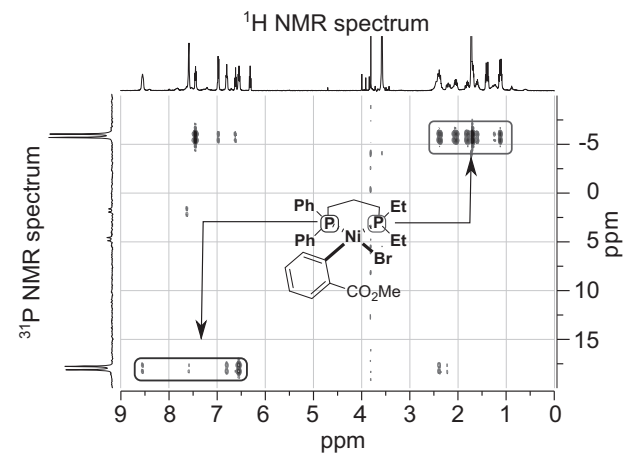
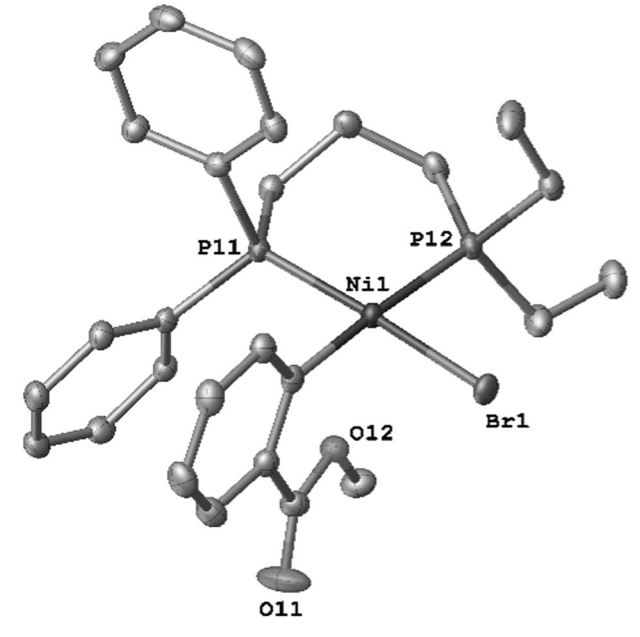


Fig. 3 Selected region of an  $^{1}H^{-31}P$  HMQC experiment (500 MHz) recorded for (sepp)Ni(o-C<sub>6</sub>H<sub>4</sub>CO<sub>2</sub>Me)Br in THF-d<sub>8</sub> at 22  $^{\circ}$ C



**Fig. 4** Solid-state molecular structure of (sepp)Ni(o-C<sub>6</sub>H<sub>4</sub>CO<sub>2</sub>Me)Br (thermal ellipsoids at 50% probability) with H atoms omitted. Only one of the two independent molecules is shown

X-ray diffraction (Fig. 4). There are two independent molecules in the unit cell (similar to Ni(sepp)Cl<sub>2</sub>). In the solid-state molecular structure, the nickel–phosphine bond lengths are significantly different, and the PPh<sub>2</sub>–Ni bond *trans* to the Br is nearly 0.1 Å shorter than the PEt<sub>2</sub>–Ni bond (2.1384(4) versus 2.2277(4) Å, respectively). This was expected considering the strong σ-donating properties of the reactive arene ligand opposite the PEt<sub>2</sub> group. The average bite angle of the ligands was nearly 98° for this complex. The oxygen atom (O12) and nickel are within the sum of their Van der Waals radii but there is not a strong bonding interaction (Ni1–O12 distance is 2.545 Å).

The formation of the major isomer during the polymerization (Fig. 2), and the observation of the same preference when synthesizing a complex by ligand exchange (Figs. 3 and 4), suggests a significant energy difference with the relative orientation of the reactive arene and the bromide. The total energies of the two possible stereoisomers were calculated (3-methylthiophene was used to mimic the polymer chain), and as expected, the trans relationship of the PEt<sub>2</sub> group and the reactive ligand is favored by 3.7 kcal/mol (Fig. 5—computed structures **A** and **B**). We suspect the energy difference is due to steric constraints as more distortion from square planar geometry around the nickel is observed in A. A mean plane was constructed from four atoms for both the optimized geometries: the nickel, the two phosphines from the ligand, and the carbon atom of the 2-position for the thiophene ring. In A (the higher energy structure), the bromine atom is distorted by 0.55 Å from the plane, while this value is only 0.25 Å in **B** (lower energy structure). A picture illustrating these distortions from the mean planes is provided in Fig. S26.

Once the energy preference for the Ni<sup>2+</sup> species generated by oxidative addition was established, the two catalysts, Ni(sepp)Cl<sub>2</sub> and (sepp)Ni(o-C<sub>6</sub>H<sub>4</sub>CO<sub>2</sub>Me)Br, were used to polymerize monomer 1. The MALDI-TOF mass spectra for the P3HT samples generated using these two

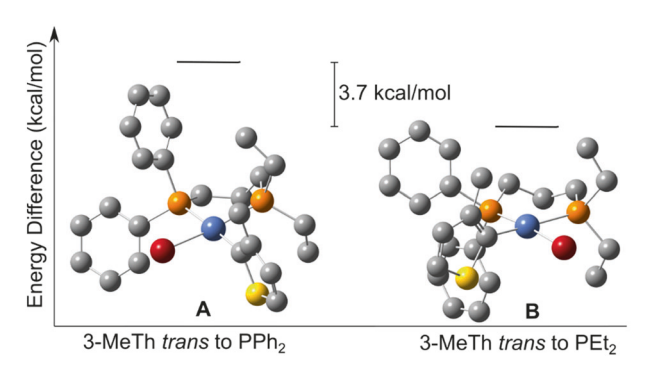
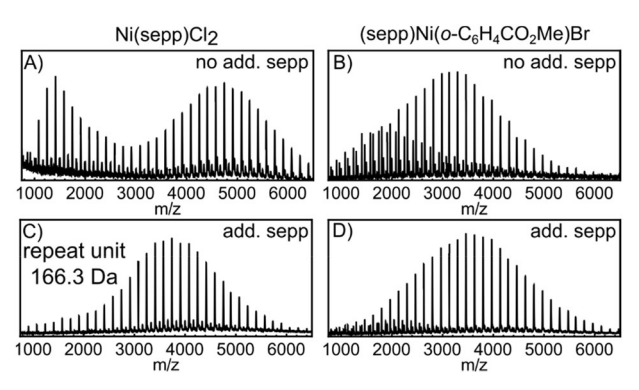


Fig. 5 DFT-optimized structures of the two possible stereoisomers of (sepp)Ni(3-methylthiophene)Br (H atoms omitted). Optimization and total energy calculations were conducted with a mixed basis set using B3LYP 6–31 G(d) for all ligand atoms and SDD for nickel

catalysts (4 mol %) revealed some interesting features. For Ni(sepp)Cl<sub>2</sub>, a tail was observed in the lower-molecularweight region (along with a minor second distribution) and for (sepp)Ni(o-C<sub>6</sub>H<sub>4</sub>CO<sub>2</sub>Me)Br, a second mass distribution was observed at lower molecular weights (Fig. 6a, b, respectively). The appearance of these lower-molecularweight species suggested unproductive side-reactions (chain-transfer or chain-chain coupling) during the polymerization. In the GPC traces, we observed highermolecular-weight shoulders in some cases, which is indicative of chain-chain coupling. This can occur when two growing chains ((sepp)Ni(polymer)Br) exchange reactive ligands producing (sepp)Ni(polymer)<sub>2</sub> and (sepp)NiBr<sub>2</sub>. Reductive elimination from (sepp)Ni(polymer)<sub>2</sub> can then produce higher-molecular-weight materials, and the resultant metal species can begin growing new chains, affording lower-molecular-weight species.

In our previous report on Suzuki–Miyaura CTPs using Ni(dppp)Cl<sub>2</sub>, catalyst hydrolysis was critical to controlling the polymerization process, as it released free ligand into the reaction mixture [25]. The free ligand does not have a significant impact on the rate of the polymerization, but it was necessary to obtain high-molecular-weight P3HT with good control over the end groups. Since Ni(sepp)Cl<sub>2</sub> and (sepp)Ni(o-C<sub>6</sub>H<sub>4</sub>CO<sub>2</sub>Me)Br are more resistant to hydrolysis, minimal free ligand is present in the reaction during the polymerization. To evaluate whether additional free ligand could improve the polymerization, sepp was added to Ni(sepp)Cl<sub>2</sub>- and (sepp)Ni(o-C<sub>6</sub>H<sub>4</sub>CO<sub>2</sub>Me)Br-initiated polymerizations (Fig. 6c, d).

The change in the MALDI-TOF mass spectra for the as-obtained P3HT samples prepared using these two different catalyst systems was remarkable. When the polymerization was conducted in the presence of additional sepp ligand, the distribution of chain lengths was in line



**Fig. 6** MALDI-TOF mass spectra for P3HT samples. **a** Ni(sepp)Cl<sub>2</sub> and **b** (sepp)Ni(o-C<sub>6</sub>H<sub>4</sub>CO<sub>2</sub>Me)Br. The spectra in **c** and **d** correspond to the same catalysts with an additional 1.0 equiv of sepp added to the reaction mixture (relative to [Ni]). The reaction conditions were as described in Table 1, entries 1, 5, 3, and 7 for **a**, **b**, **c**, and **d**, respectively

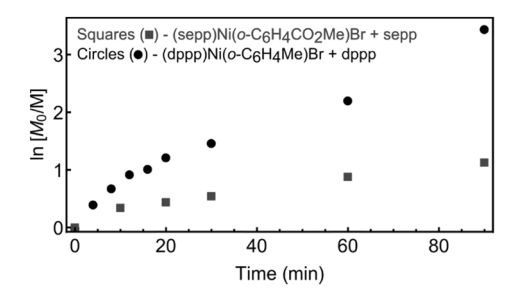
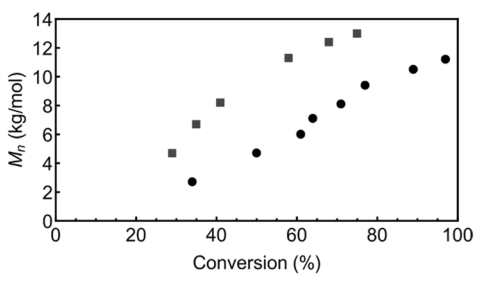


**Fig. 7** Left: semilogarithmic plot of concentration versus time. Right: number-average molecular weight versus conversion. Black circles correspond to 2 mol% (dppp)Ni(o-C<sub>6</sub>H<sub>4</sub>Me)Br with dppp, and blue squares correspond to 2 mol% (sepp)Ni(o-C<sub>6</sub>H<sub>4</sub>CO<sub>2</sub>Me)Br with sepp.

with a living polymerization (Poisson distribution) (Fig. 6c, d). Very minor secondary distributions were observed in both spectra, indicating that although the polymerization is not perfect, additional ligand greatly improves the control over the end groups (see the integrations of the P3HT samples in the ESI) and the molecular weight distribution. For reference, the molecular weight data from GPC and NMR are included in Table 1.

A molecular weight versus conversion plot and a semilogarithmic plot were generated for (sepp)Ni(o-C<sub>6</sub>H<sub>4</sub>CO<sub>2</sub>Me) Br in the presence of additional sepp ligand. This experiment was completed in an identical manner to our previous report though different time intervals were used [25]. The collected data were then compared to those of (dppp)Ni(o-tolyl)Br with additional dppp (Fig. 7) [25]. As expected, the profile is very similar to that of the dppp system, but the newly synthesized catalyst produces the polymer at a slower rate. In both semilog plots, deviations from linearity were observed, similar to the 3-hexylthiophene polymerization using a Kumada coupling [58]. As such, no rate constants were extracted; however, qualitatively, it is clear that (dppp)Ni is faster. As expected, the  $M_{\rm n}$  values increase for both catalysts with conversion, although they both begin to level off at higher conversions. This is indicative of chain-transfer towards the end of the polymerization, which could be a result of repeated sampling because the dispersity of the final polymer samples was higher (~1.15) than in the isolated polymerizations presented in Table 1 (entries 7 and 8).

Ultimately, the additional ligand clearly has a positive impact on the polymerization. Miyaura proposed in prior work that free ligand stabilizes Ni(0) [50–52, 59], and Van Der Boom has illustrated that additional phosphine ligand can suppress intermolecular pathways in aryl halide bond activations with platinum species [60]. These reports highlight the importance of free ligands for improving catalyst lifetime and chain fidelity, respectively. Future work will explore this effect in more detail to better elucidate how free ligand exerts this positive effect.



For both polymerizations, [1] was 25 mM in THF with 0.5 mM catalyst and ligand. The (dppp)Ni experimental data was taken directly from ref. [25]

## **Conclusions**

In conclusion, we have prepared a new, unsymmetrical nickel diphosphine catalyst for CTP. The diphosphine comprises two electronically and sterically distinct moieties, one PPh<sub>2</sub> group and one stronger σ-donating PEt<sub>2</sub> group. The nickel catalyst retains one ligand site that is identical to the highly successful Ni(dppp) system, while offering another donor in the scaffold as a tunable site. Ni(sepp)Cl<sub>2</sub> proved to be an excellent catalyst for the controlled polymerization of an organoboron precursor if excess free ligand is present in the reaction mixture. The P3HT obtained using this catalyst system is essentially identical to that obtained using Ni(dppp)Cl<sub>2</sub>.

This work, as well as our prior efforts, are consistent with the reports from Yokozawa et al. [61], McNeil and coworkers [62], and Choi and co-workers [14] who have noted the benefits of free ligand in CTP reactions. Lee and Luscombe [63] have also noted the importance of additional pyridine in recent studies on chain-growth polymerizations via direct arylation. In the future, we will explore other classes of unsymmetrical diphosphines for CTP. Additionally, the Ni(sepp)Cl<sub>2</sub> system and the externally initiated variant will be evaluated as catalysts for the polymerization of other monomers using Suzuki–Miyaura CTPs.

Acknowledgements K.J.T.N. is grateful to the NSF for a CAREER Award (CHE-1455136). The NMR instrumentation at Carnegie Mellon University is partially supported by the NSF (CHE-0130903, CHE-1039870, and CHE-1726525). The authors would also like to thank both Prof. Tsutomu Yokozawa and Prof. Anne McNeil for helpful discussions.

# Compliance with ethical standards

Conflict of interest The authors declare that they have no conflict of interest.

**Publisher's note:** Springer Nature remains neutral with regard to jurisdictional claims in published maps and institutional affiliations.

#### References

- He WY, Patrick BO, Kennepohl P. Identifying the missing link in catalyst transfer polymerization. Nat Commun. 2018;9:3866.
- Leone AK, Goldberg PK, McNeil AJ. Ring-walking in catalysttransfer polymerization. J Am Chem Soc. 2018;140:7846–50.
- Baker MA, Tsai CH, Noonan KJT. Diversifying cross-coupling strategies, catalysts and monomers for the controlled synthesis of conjugated polymers. Chem Eur J. 2018;24:13078–88.
- Verheyen L, Leysen P, Van den Eede M-P, Ceunen W, Hardeman T, Koeckelberghs G. Advances in the controlled polymerization of conjugated polymers. Polymer. 2017;108:521

  –46.
- Yokozawa T, Ohta Y. Transformation of step-growth polymerization into living chain-growth polymerization. Chem Rev. 2016;116:1950–68.
- Leone AK, McNeil AJ. Matchmaking in catalyst-transfer polycondensation: optimizing catalysts based on mechanistic insight. Acc Chem Res. 2016;49:2822–31.
- Bryan ZJ, McNeil AJ. Conjugated polymer synthesis via catalysttransfer polycondensation (CTP): mechanism, scope, and applications. Macromolecules. 2013;46:8395

  –405.
- Okamoto K, Luscombe CK. Controlled polymerizations for the synthesis of semiconducting conjugated polymers. Polym Chem. 2011;2:2424–34.
- Yokozawa T, Yokoyama A. Chain-growth condensation polymerization for the synthesis of well-defined condensation polymers and π-conjugated polymers. Chem Rev. 2009;109:5595–619.
- Grisorio R, Suranna GP. Intramolecular catalyst transfer polymerisation of conjugated monomers: from lessons learned to future challenges. Polym Chem. 2015;6:7781–95.
- Leone AK, Mueller EA, McNeil AJ. The history of palladiumcatalyzed cross-couplings should inspire the future of catalysttransfer polymerization. J Am Chem Soc. 2018;140:15126–39.
- Sugita H, Nojima M, Ohta Y, Yokozawa T. Unstoichiometric Suzuki–Miyaura cyclic polymerization of extensively conjugated monomers. Polym Chem. 2019;10:1182–5.
- Kosaka K, Uchida T, Mikami K, Ohta Y, Yokozawa T. AmPhos Pd-catalyzed Suzuki Miyaura catalyst-transfer condensation polymerization: narrower dispersity by mixing the catalyst and base prior to polymerization. Macromolecules. 2018;51:364–9.
- 14. Seo K-B, Lee I-H, Lee J, Choi I, Choi T-L. A rational design of highly controlled Suzuki-Miyaura catalyst-transfer polycondensation for precision synthesis of polythiophenes and their block copolymers: marriage of palladacycle precatalysts with MIDA-boronates. J Am Chem Soc. 2018;140:4335–43.
- Sugita H, Nojima M, Ohta Y, Yokozawa T. Unusual cyclic polymerization through Suzuki–Miyaura coupling of polyphenylene bearing diboronate at both ends with excess dibromophenylene. Chem Commun. 2017;53:396–9.
- Grisorio R, Suranna GP. Impact of precatalyst activation on Suzuki-Miyaura catalyst-transfer polymerizations: new mechanistic scenarios for pre-transmetalation events. ACS Macro Lett. 2017;6:1251–6.
- 17. Zhang H-H, Peng W, Dong J, Hu Q-S. *t*-Bu<sub>3</sub>P-coordinated 2-Phenylaniline-based palladacycle complex/ArBr as robust initiators for controlled Pd(0)/*t*-Bu<sub>3</sub>P-catalyzed Suzuki crosscoupling polymerization of AB-type monomers. ACS Macro Lett. 2016;5:656–60.
- Zhang H-H, Xing C-H, Hu Q-S, Hong K. Controlled Pd(0)/t-Bu<sub>3</sub>P-catalyzed Suzuki cross-coupling polymerization of AB-type monomers with ArPd(t-Bu<sub>3</sub>P)X or Pd<sub>2</sub>(dba)<sub>3</sub>/t-Bu<sub>3</sub>P/ArX as the initiator. Macromolecules. 2015;48:967–78.
- Kosaka K, Ohta Y, Yokozawa T. Influence of the boron moiety and water on Suzuki-Miyaura catalyst-transfer condensation polymerization. Macromol Rapid Commun. 2015;36:373–7.

- Sui A, Shi X, Tian H, Geng Y, Wang F. Suzuki-Miyaura catalysttransfer polycondensation with Pd(IPr)(OAc)2 as the catalyst for the controlled synthesis of polyfluorenes and polythiophenes. Polym Chem. 2014;5:7072–80.
- Grisorio R, Mastrorilli P, Suranna GP. A Pd(AcO)<sub>2</sub>/t-Bu<sub>3</sub>P/K<sub>3</sub>PO<sub>4</sub> catalytic system for the control of Suzuki cross-coupling polymerisation. Polym Chem. 2014;5:4304–10.
- 22. Zhang H-H, Xing C-H, Hu Q-S. Controlled Pd(0)/t-Bu<sub>3</sub>P-catalyzed Suzuki cross-coupling polymerization of AB-type monomers with PhPd(t-Bu<sub>3</sub>P)I or Pd<sub>2</sub>(dba)<sub>3</sub>/t-Bu<sub>3</sub>P/ArI as the initiator. J Am Chem Soc. 2012;134:13156–9.
- Yokozawa T, Suzuki R, Nojima M, Ohta Y, Yokoyama A. Precision synthesis of poly(3-hexylthiophene) from catalyst-transfer Suzuki—Miyaura coupling polymerization. Macromol Rapid Commun. 2011;32:801–6.
- Yokoyama A, Suzuki H, Kubota Y, Ohuchi K, Higashimura H, Yokozawa T. Chain-growth polymerization for the synthesis of polyfluorene via Suzuki-Miyaura coupling reaction from an externally added initiator unit. J Am Chem Soc. 2007;129:7236-7.
- Baker MA, Zahn SF, Varni AJ, Tsai CH, Noonan KJT. Elucidating the role of diphosphine ligand in nickel-mediated Suzuki-Miyaura polycondensation. Macromolecules. 2018;51:5911–7.
- Qiu Y, Worch JC, Fortney A, Gayathri C, Gil RR, Noonan KJT. Nickel-catalyzed Suzuki polycondensation for controlled synthesis of ester-functionalized conjugated polymers. Macromolecules. 2016;49:4757–62.
- Benn FR, Briggs JC, McAuliffe CA. Unsymmetrical bis (phosphorus) compounds: synthesis of unsymmetrical ditertiary phosphines, phosphine oxides, and diquaternary phosphonium salts. J Chem Soc Dalton Trans. 1984:293–5.
- Briggs JC, McAuliffe CA, Hill WE, Minahan DMA, Dyer G. Unsymmetrical bisphosphorus ligands - Phosphorus-31 and Carbon-13 nuclear magnetic-resonance and mass-spectral measurements. J Chem Soc Perkin Trans 2. 1982:321–5.
- 29. Briggs JC, Dyer G. New synthesis of unsymmetrical bidendate phosphine ligands. Chem Ind. 1982:163–4.
- Petit C, Favre-Reguillon A, Albela B, Bonneviot L, Mignani G, Lemaire M. Mechanistic Insight into the reduction of tertiary phosphine oxides by Ti(OiPr)<sub>4</sub>/TMDS. Organometallics. 2009; 28:6379–82.
- Liversedge IA, Higgins SJ, Giles M, Heeney M, McCulloch I. Suzuki route to regioregular polyalkylthiophenes using Ircatalysed borylation to make the monomer, and Pd complexes of bulky phosphanes as coupling catalysts for polymerisation. Tetrahedron Lett. 2006;47:5143–6.
- Harris RK, Becker ED, De Menezes SMC, Goodfellow R, Granger P. NMR nomenclature. Nuclear spin properties and conventions for chemical shifts (IUPAC recommendations 2001). Pure Appl Chem. 2001;73:1795–818.
- 33. CrysAlisPro; The Woodlands, TX: Rigaku OD; 2015.
- 34. Sheldrick G. SHELXT—integrated space-group and crystal-structure determination. Acta Cryst Sec A. 2015;71:3–8.
- Sheldrick G. A short history of SHELX. Acta Cryst Sec A. 2008;64:112–22.
- Müller P. Practical suggestions for better crystal structures. Crystallogr Rev. 2009;15:57–83.
- 37. Kohn P, Huettner S, Komber H, Senkovskyy V, Tkachov R, Kiriy A, et al. On the role of single regiodefects and polydispersity in regioregular poly(3-hexylthiophene): defect distribution, synthesis of defect-free chains, and a simple model for the determination of crystallinity. J Am Chem Soc. 2012;134:4790–805.
- Bronstein HA, Luscombe CK. Externally initiated regioregular P3HT with controlled molecular weight and narrow polydispersity. J Am Chem Soc. 2009;131:12894–5.
- 39. Iovu MC, Sheina EE, Gil RR, McCullough RD. Experimental evidence for the quasi-"living" nature of the Grignard metathesis

method for the synthesis of regioregular poly(3-alkylthiophenes). Macromolecules. 2005;38:8649–56.

- Frisch MJ, Trucks GW, Schlegel HB, Scuseria GE, Robb MA, Cheeseman JR, et al. Gaussian 09. Gaussian, Inc., Wallingford, CT: Gaussian, Inc.; 2009.
- 41. Pople JA. The effect of quadrupole relaxation on nuclear magnetic resonance multiplets. Mol Phys. 1958;1:168–74.
- 42. Bomfim JAS, de Souza FP, Filgueiras CAL, de Sousa AG, Gambardella MTP. Diphosphine complexes of nickel: analogies in molecular structures and variety in crystalline arrangement. Polyhedron. 2003;22:1567–73.
- 43. Thomas AA, Zahrt AF, Delaney CP, Denmark SE. Elucidating the role of the boronic esters in the Suzuki–Miyaura reaction: structural, kinetic, and computational investigations. J Am Chem Soc. 2018;140:4401–16.
- Thomas AA, Denmark SE. Pre-transmetalation intermediates in the Suzuki-Miyaura reaction revealed: the missing link. Science. 2016;352:329–32.
- Lennox AJJ, Lloyd-Jones GC. Transmetalation in the Suzuki-Miyaura coupling: the fork in the trail. Angew Chem Int Ed. 2013;52:7362-70.
- Carrow BP, Hartwig JF. Distinguishing between pathways for transmetalation in Suzuki-Miyaura reactions. J Am Chem Soc. 2011;133:2116–9.
- 47. Amatore C, Jutand A, Le Duc G. Kinetic data for the transmetalation/reductive elimination in palladium-catalyzed Suzuki-Miyaura reactions: unexpected triple role of hydroxide ions used as base. Chem Eur J. 2011;17:2492–503.
- 48. Schmidt AF, Kurokhtina AA, Larina EV. Role of a base in Suzuki-Miyaura reaction. Russ J Gen Chem. 2011;81:1573.
- Christian AH, Muller P, Monfette S. Nickel hydroxo complexes as intermediates in nickel-catalyzed Suzuki-Miyaura cross-coupling. Organometallics. 2014;33:2134–7.
- Inada K, Miyaura N. Synthesis of biaryls via crosscoupling reaction of arylboronic acids with aryl chlorides catalyzed by NiCl<sub>2</sub>/triphenylphosphine complexes. Tetrahedron. 2000;56:8657–60.
- Ueda M, Saitoh A, Oh-tani S, Miyaura N. Synthesis of biaryls via nickel-catalyzed cross-coupling reaction of arylboronic acids and aryl mesylates. Tetrahedron. 1998;54: 13079–86.

- Saito S, Oh-tani S, Miyaura N. Synthesis of biaryls via a nickel (0)-catalyzed cross-coupling reaction of chloroarenes with arylboronic acids. J Org Chem. 1997;62:8024–30.
- Lanni EL, McNeil AJ. Evidence for ligand-dependent mechanistic changes in nickel-catalyzed chain-growth polymerizations. Macromolecules. 2010;43:8039

  –44.
- Senkovskyy V, Sommer M, Tkachov R, Komber H, Huck WTS, Kiriy A. Convenient route to initiate Kumada catalyst-transfer polycondensation using Ni(dppe)Cl<sub>2</sub> or Ni(dppp)Cl<sub>2</sub> and sterically hindered Grignard compounds. Macromolecules. 2010;43:10157–61.
- Senkovskyy V, Tkachov R, Beryozkina T, Komber H, Oertel U, Horecha M, et al. "Hairy" poly(3-hexylthiophene) particles prepared via surface-initiated Kumada catalyst-transfer polycondensation. J Am Chem Soc. 2009:131:16445–53.
- Boyd SD, Jen AK-Y, Luscombe CK. Steric stabilization effects in nickel-catalyzed regioregular poly(3-hexylthiophene) synthesis. Macromolecules. 2009;42:9387–9.
- Doubina N, Ho A, Jen AK-Y, Luscombe CK. Effect of initiators on the Kumada catalyst-transfer polycondensation reaction. Macromolecules. 2009;42:7670–7.
- Sheina EE, Liu J, Iovu MC, Laird DW, McCullough RD. Chain growth mechanism for regioregular nickel-initiated cross-coupling polymerizations. Macromolecules. 2004;37:3526–8.
- Saito S, Sakai M, Miyaura N. A synthesis of biaryls via nickel(0)catalyzed cross-coupling reaction of chloroarenes with phenylboronic acids. Tetrahedron Lett. 1996;37:2993–6.
- Zenkina O, Altman M, Leitus G, Shimon LJW, Cohen R, van der Boom ME. From azobenzene coordination to aryl-halide bond activation by platinum. Organometallics. 2007;26:4528–34.
- 61. Yokoyama A, Kato A, Miyakoshi R, Yokozawa T. Precision synthesis of poly (N-hexylpyrrole) and its diblock copolymer with poly(p-phenylene) via catalyst-transfer polycondensation. Macromolecules. 2008;41:7271–3.
- Hall AO, Lee SR, Bootsma AN, Bloom JWG, Wheeler SE, McNeil AJ. Reactive ligand influence on initiation in phenylene catalyst-transfer polymerization. J Polym Sci Part A Polym Chem. 2017;55:1530–5.
- Lee JA, Luscombe CK. Dual-catalytic Ag-Pd system for direct arylation polymerization to synthesize poly(3-hexylthiophene). ACS Macro Lett. 2018;7:767–71.